ACS chemical biology

Articles

pubs.acs.org/acschemicalbiology

Position of Proline Mediates the Reactivity of S-Palmitoylation

Neelam Khanal,[†] Vikas Pejaver,[‡] Zhiyu Li,[†,∥] Predrag Radivojac,[‡] David E. Clemmer,[*,†] and Suchetana Mukhopadhyay[*,§]

Departments of [†]Chemistry, [‡]Computer Science and Informatics, and [§]Biology, Indiana University, Bloomington, Indiana 47405, United States

Supporting Information

ABSTRACT: Palmitoylation, a post-translational modification in which a saturated 16-carbon chain is added predominantly to a cysteine residue, participates in various biological functions. The position of proline relative to other residues being post-translationally modified has been previously reported as being important. We determined that proline is statistically enriched around cysteines known to be S-palmitoylated. The goal of this work was to determine how the position of proline influences the palmitoylation of the cysteine residue. We established a mass spectrometry-based approach to investigate time- and temperature-dependent kinetics of autopalmitoylation *in vitro* and to derive the thermodynamic parameters of the transition state associated with palmitoylation; to the best of our knowledge, our work is the first to study the kinetics and activation properties of the palmitoylation process. We then used these thermochemical parameters to determine if the position of proline relative to the modified cysteine is important for palmitoylation. Our results show that peptides with proline at the −1 position of cysteine in their sequence (PC) have lower enthalpic barriers and higher entropic barriers in comparison to the same peptides with proline at the +1 position of cysteine (CP); interestingly, the free-energy barriers for both pairs are almost identical. Molecular dynamics studies demonstrate that the flexibility of the cysteine backbone in the PC-containing peptide when compared to the CP-containing peptide explains the increased entropic barrier and decreased enthalpic barrier observed experimentally.

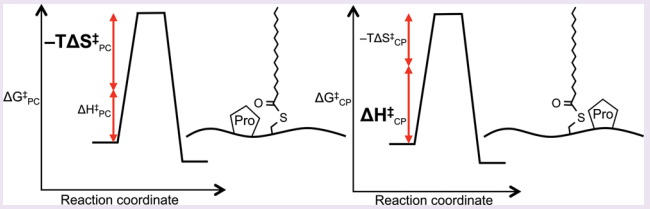

Post-translational modifications (PTMs) are critical for regulating the spatial and temporal localization of proteins within a cell, which in turn dictates their activity individually or as complexes.[1,2] S-palmitoylation is a type of PTM which couples a 16-carbon acyl chain to the cysteine side chain of a protein and regulates a multitude of cellular processes.[3−5] Depalmitoylation, a process of removal of the acyl chain, is equally important in maintaining biological homeostasis. Misbalance between palmitoylation and depalmitoylation results in proteins not being palmitoylated at the proper time and locale, and has been implicated in different neurological diseases, including Huntington disease, Alzheimer's disease, and Parkinson's disease.[6]

In vivo, a family of enzymes called palmitoyl acyltransferases (PATs) and palmitoyl thioesterases have been identified to palmitate and depalmitate cellular proteins, respectively.[5,7−10] Many proteins are known to autoacylate (autopalmitoylation) in the presence of palmitoyl-CoA (Pal-CoA), which adds to the complexity in defining the requirements for palmitoylation.[11,12] In humans, there are up to 23 PATs, yet the mechanism that regulates which PAT modifies which protein substrate is unclear. No conserved structural domain or sequence motif at the site of S-palmitoylation has been identified.[13,14] In general, most palmitoylated cysteines are found within regions close to the transmembrane domain (TMD)[15−17] of proteins or in loop regions of proteins.[18−22] Palmitoylated cysteines are often adjacent to either basic or hydrophobic residues,[16] but these neighboring residues can have different effects on the state of palmitoylation. For example, in postsynaptic density-95 (PSD-95/SAP-90), the presence of hydrophobic residues near cysteine promotes its palmitoylation;[23] however, in influenza virus hemagglutinin A (HA), hydrophobic residues close to the cysteine deter palmitoylation.[24]

For other PTMs such as O- and N-linked glycosylation and phosphorylation, the position of proline with respect to the modified residue is critical.[25−30] From examining the literature and public databases, we identified 396 known palmitoylation sites from different proteins in multiple species. Of these, 361 were annotated as S-palmitoylation sites. From these 361 known modified sites, 15.2% (55 sites) had a proline residue in either the −1 or +1 position (Supplementary Table 1). In contrast, cysteines that were not annotated as being S-palmitoylated in the same set of proteins had proline residues in the −1 or +1 position in 9.6% of the samples. Given the importance of proline positioning in other PTMs and its influence on peptide/protein structure,[31,32] we were interested to see how the location of proline relative to cysteine is important in S-palmitoylation.

In this work, we determined how the position of proline affects autopalmitoylation *in vitro*. We established a mass

Received: June 3, 2015
Accepted: August 9, 2015

DOI: 10.1021/acschembio.5b00429
ACS Chem. Biol. XXXX, XXX, XXX−XXX

spectrometry (MS)-based approach to determine the kinetics and thermodynamic activation parameters that influence *in vitro* autopalmitoylation. We identified known palmitoylated proteins that contain a proline residue adjacent to the palmitoylated cysteine. We synthesized a peptide corresponding to the region of palmitoylation and another peptide with the same sequence, but the position of proline was swapped with the residue at +1 or −1 position relative to the cysteine. We find that despite similar values of Gibbs free energy of activation, enthalpic and entropic contributions to free energy are different for these peptide pairs. The structural properties of PC and CP peptides, obtained from molecular dynamics simulations, provide additional insights into their thermodynamic properties. This work provides the basis for understanding enzymatic S-palmitoylation of proteins that occurs *in vivo*.

RESULTS AND DISCUSSION

Kinetics of Palmitoylation via MS. MS-based methods have been implemented to identify modification sites in proteins and to probe enzyme kinetics governing various PTMs.[33−35] MS-based approaches can also be useful to perform kinetics measurements with respect to time and temperature for various PTMs because of their ability to measure both unmodified and modified proteins (peptides) simultaneously.[36,37] To establish that the kinetics of palmitoylation could be studied via mass spectrometry, we first monitored the palmitoylation of a single peptide, LLFGPCILNR. This sequence is present in the transmembrane domain of the envelope protein in the Friend strain of murine leukemia virus. Previous studies have shown that the cysteine residue (Cys606) is palmitoylated and is critical for lipid raft association and surface expression.[38,39] In our study, we used Pal-CoA to add a palmitate group to the cysteine residue (underlined) in the peptide LLFGPCILNR (Figure 1).

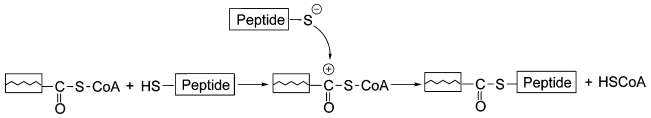

Figure 1. Mechanism for autopalmitoylation. Peptide backbone and palmitate group are represented in the boxes containing the word "Peptide" and broken lines, respectively.

The peptide LLFGPCILNR was incubated with Pal-CoA, and at different times, aliquots of the reaction mixture were desalted by solid phase extraction and were analyzed by MS. A representative example of mass spectra for the peptide LLFGPCILNR is shown in Figure 2a (Supplementary Figure S1 shows entire spectra). The mass spectrum obtained at 0 h (bottom panel), before addition of Pal-CoA, is dominated by a single peak corresponding to $[M + 2H]^{2+}$ ion of the peptide (m/z = 573.3). The mass spectrum obtained after addition of Pal-CoA at 0.25 h shows a new peak (m/z = 692.4) along with the precursor peak of the peptide ion. Mass addition of ∼238 (an increase of 119 in m/z for a + 2 ion) between two peaks suggests that the new peak corresponds to the peptide with palmitoylated cysteine. The palmitoylated peptide peak is denoted as $[M^* + 2H]^{2+}$ in Figure 2a. Mass spectra obtained at 0.75, 1, 1.25, 1.5, and 1.75 h show how the palmitoylated peptide peak increases while the precursor peptide peak depletes over time (Figure 2a).

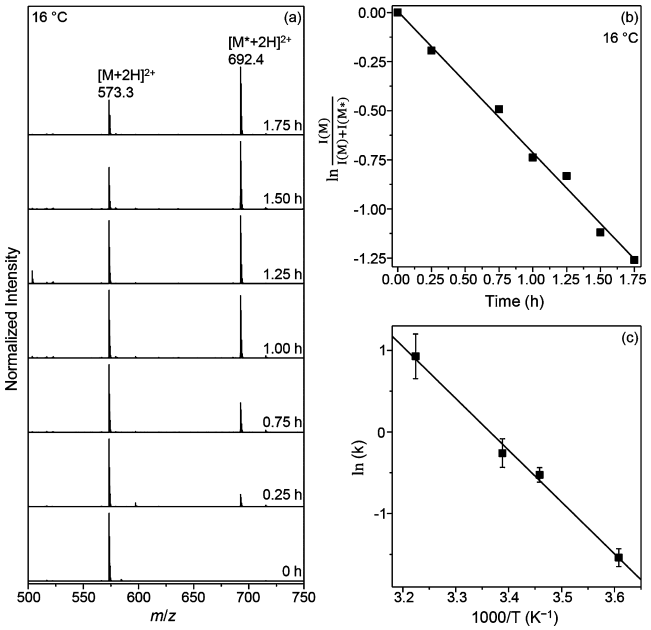

Figure 2. LLFGPCILNR kinetics as a function of time and temperature. (a) Mass spectra acquired at different times from the reaction mixture incubated at 16 °C. Spectra are arranged in increasing order of time from bottom to top. Unmodified peptide peak and palmitoylated peptide peak are denoted as $[M + 2H]^{2+}$ and $[M^* + 2H]^{2+}$ respectively. (b) Representative linear plot for logarithmic ratio of intensities (unmodified peptide to sum of unmodified and modified peptide) as a function of time. Slope of the line provides rate constant (k) for the reaction (c) Arrhenius plot obtained from rate constants at four different temperatures. Measurement of rate constant at all temperatures is performed in triplicates. The error bars represent the standard deviation of the measurements.

We analyzed how the ratio of precursor peptide (total counts of monoisotopic peak for the unmodified peptide) to both modified and unmodified peptide (sum of total counts for monoisotopic peaks of both modified and unmodified peptide) decreased over time. When the logarithmic function of this ratio is plotted with respect to time, a straight line is produced (Figure 2b), and when the ratio of intensities is plotted as a function of time, the line fits to an exponential curve (Supplementary Figure S2), both indicating that the reaction follows pseudo first-order kinetics. Lastly, there was no change in the ratio (unmodified peptide to the sum of modified and unmodified peptide) when the concentration of the peptide in the reaction mixture was changed, consistent with a pseudo first-order reaction. The slope of the line obtained from Figure 2b corresponds to rate-constant (k) of the reaction at a particular temperature.

We determined the rate-constant for palmitoylation at four different temperatures. A representative example of an Arrhenius plot, obtained by plotting ln k with $1/T$ for peptide LLFGPCILNR, is depicted in Figure 2c. From the slope of the plot, we determined the value of the energy barrier (E_a) for the reaction (Table 1), which corresponds to the minimum energy needed for the reaction to proceed. The Arrhenius eq eq 1 establishes a relation between rate constant (k) and temperature (T).

$$k = Ae^{-E_a/RT} \quad (1)$$

where A is the pre-exponential factor, R is the ideal gas constant, and T is the temperature in Kelvin.

DOI: 10.1021/acschembio.5b00429
ACS Chem. Biol. XXXX, XXX, XXX−XXX

Table 1. Thermodynamic Activation Parameters for Autopalmitoylation of Peptides

	UniProt ID	peptide sequence		E_a (kJ·mol^{-1})	$\Delta H^{\ddagger,a}$ (kJ·mol^{-1})	$\Delta S^{\ddagger,a}$ (J·mol^{-1}·K)	$\Delta G^{\ddagger,a}$ (kJ·mol^{-1})
P1	ENV_MLVF5	original	LLFGPCILNR	53 ± 2	50 ± 2	−68 ± 7	71 ± 0
		swapped	LLFGICPLNR	94 ± 4	92 ± 4	61 ± 15	73 ± 0
		shuffled	LIGPNCFLLR	66 ± 2	63 ± 2	−29 ± 7	72 ± 0
P2	PSPC_CANFA	original	GIPCFPSSLK	46 ± 1	44 ± 1	−118 ± 4	80 ± 0
		swapped	GIFCPPSSLK	113 ± 2	110 ± 2	90 ± 6	82 ± 0
		shuffled	SGFCISPLPK	61 ± 3	58 ± 3	−63 ± 8	78 ± 0
P3[b]	RPE65_CYNPY	original	VVVQFPCSER	62 ± 3	59 ± 3	−75 ± 9	83 ± 0
		swapped	VVVQFSCPER	89 ± 3	87 ± 3	−7 ± 10	89 ± 0
		shuffled	PVESVFCQVR	72 ± 2	70 ± 2	−65 ± 7	90 ± 0
P4	MA6D1_HUMAN	original	MAWPCISR	54 ± 3	51 ± 3	−81 ± 10	76 ± 0
		swapped	MAWICPSR	77 ± 4	74 ± 4	−21 ± 14	80 ± 0
		shuffled	APWSCMIR	66 ± 3	63 ± 3	−42 ± 11	76 ± 0
P5	SNP23_HUMAN	original	GGENSPCNVVSK	59 ± 5	57 ± 5	−79 ± 16	81 ± 0
		swapped	GGENSNCPVVSK	76 ± 3	73 ± 3	−26 ± 11	81 ± 0
		shuffled	GNNSESCGPVVK	106 ± 17	103 ± 17	63 ± 53	83 ± 1
P6[c]	LRP6_HUMAN	original	MLCPR	72 ± 3	69 ± 3	−32 ± 11	79 ± 0
		swapped	MPCLR	59 ± 1	56 ± 1	−69 ± 2	78 ± 0
		shuffled	PLCMR	78 ± 3	76 ± 3	−14 ± 8	80 ± 0
P7[c]	KCNA1_HUMAN	original	FFACPSK	62 ± 2	59 ± 2	−66 ± 6	80 ± 0
		swapped	FFPCASK	48 ± 2	45 ± 2	−102 ± 8	77 ± 0
		shuffled	FPSCFAK	81 ± 6	78 ± 6	−15 ± 17	83 ± 1
P8[c]	DRD1_HUMAN	original	LCPATNNAIET	87 ± 3	84 ± 3	13 ± 11	81 ± 0
		swapped	PCLATNNAIET	63 ± 1	61 ± 1	−70 ± 3	82 ± 0
		shuffled	NCAALTNIEPT	95 ± 21	93 ± 21	25 ± 66	85 ± 1

[a]The values are calculated at 310 K. [b]Homologous sequence to actual palmitoylation site. [c]Original site is a CP sequence.

We derived the thermodynamic activation parameters ($\Delta G^{\ddagger}$, $\Delta H^{\ddagger}$, $\Delta S^{\ddagger}$) of the activated complex formed in the transition state from eqs 2, 3, and 4, respectively, as

$$\Delta H^{\ddagger} = E_a - RT \tag{2}$$

$$A = \frac{k_B T}{h} e^{\Delta S^{\ddagger}/R} \tag{3}$$

$$\Delta G^{\ddagger} = \Delta H^{\ddagger} - T\Delta S^{\ddagger} \tag{4}$$

where k_B is the Boltzmann's constant, T is the temperature in Kelvin, h is the Planck's constant, and R is the ideal gas constant. Experimental values of $\Delta H^{\ddagger}$, $\Delta S^{\ddagger}$, and $\Delta G^{\ddagger}$ at 310 K corresponding to peptide LLFGPCILNR are reported in Table 1. This detailed analysis on peptide LLFGPCILNR established that MS can be successfully implemented to study kinetics and thermodynamics of the transition state for autopalmitoylation.

Peptides with Proline Adjacent to a Palmitoylated Cysteine. We extended our kinetic analysis to study peptide sequences that correspond to known palmitoylation sites in different eukaryotic proteins. Briefly, we started with a data set of 396 experimentally determined palmitoylation sites compiled from various public databases and literature sources, covering several different species.[40] Among these sites, 361 were cysteine residues annotated as being S-palmitoylated (Supplementary Table 1). Fifty-five of these modified cysteines have proline at position −1 (PC in sequence) or +1 (CP in sequence). In order to identify peptides amenable to MS analysis, we simulated tryptic digestion around these sites and computationally extracted subsequences with only one palmitoylation site between two basic residues. In the extracted set, 22 peptides contained a PC or CP sequence; however, only 15 peptides had unique sequences that were sufficiently dissimilar from each other. Seven peptides were excluded from the study because of experimental issues including the presence of a terminal cysteine, low yield of synthesized peptide, and extremely slow rate of palmitoylation, even at high temperatures. Thus, including LLFGPCILNR, the final list used for our study consisted of eight peptides (listed as original in Table 1). Proline is present in the −1 position (PC sequence) for five peptides (P1−P5) and in the +1 position (CP sequence) for three peptides (P6−P8). We note that in the case of P1, P5, and P8, truncated versions of the original tryptic peptides were synthesized because the original sequences were too long for successful synthesis. To observe how the presence of proline in the +1 and −1 position of cysteine influenced the palmitoylation reaction, control peptides (listed as swapped in Table 1) were generated by swapping proline with the residue present in the +1 or −1 position relative to the cysteine in the original peptide to generate a PC and CP pair for each peptide. The rest of the peptide sequence remained the same.

Proline Affects the Thermochemistry of the Transition State. Arrhenius plots obtained for all eight pairs of PC and CP peptide sequences (the original and swapped) are represented in Figure 3a. In all cases, the slopes of Arrhenius plots for the CP peptides are steeper than those of the PC peptides (Figure 3a). The higher slope value for the CP peptide is indicative of a higher energy barrier for palmitoylation. The values of energy barrier (E_a) as well as thermodynamic activation parameters ($\Delta H^{\ddagger}$, $\Delta S^{\ddagger}$, and $\Delta G^{\ddagger}$) at 310 K for the eight peptide pairs are provided in Table 1 and Supplementary Table 2.

Comparisons of $\Delta H^{\ddagger}$, $\Delta S^{\ddagger}$, and $\Delta G^{\ddagger}$ values for PC and CP peptide pairs are displayed as bar graphs in Figure 3b−d. While $\Delta H^{\ddagger}$ and $\Delta S^{\ddagger}$ values for all PC and CP peptide pairs vary (Figure 3b,c), $\Delta G^{\ddagger}$ values are relatively constant for both pairs (Figure 3d, with $P = 0.14$; binomial test comparing PC and CP peptides). Most notably, all the peptides that have PC in their

DOI: 10.1021/acschembio.5b00429
ACS Chem. Biol. XXXX, XXX, XXX−XXX

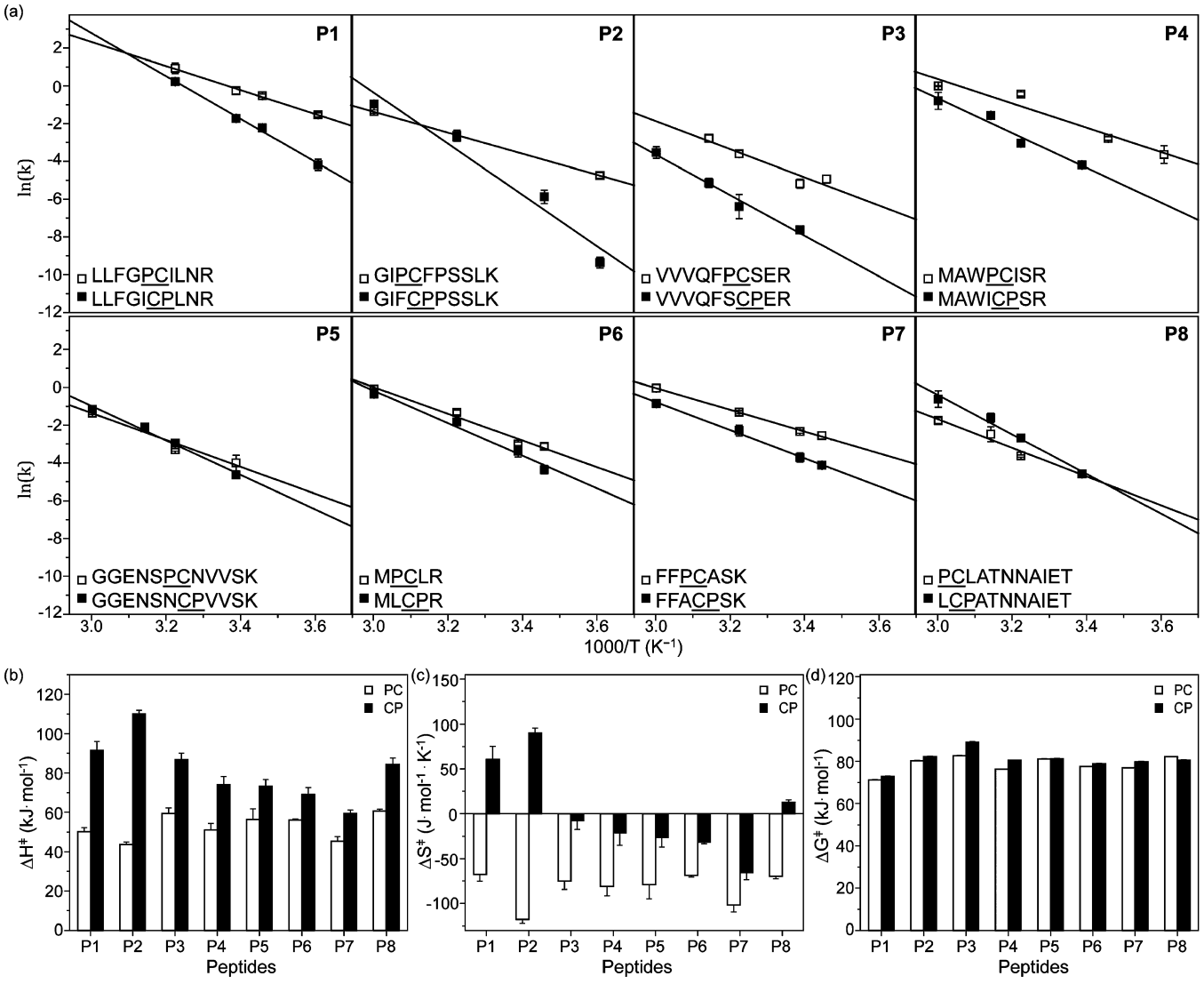

Figure 3. Kinetics and thermodynamics measurements of the transition state for PC and CP peptides. (a) Arrhenius plot for eight peptide pairs. Peptide sequences are shown and PC and CP sequences are represented by (□) and (■) respectively. (b–d) Bar graphs to compare enthalpy, entropy, and free energy of activation at 310 K corresponding to PC (white) and CP (black) peptide sequences, respectively. All measurements of rate constant are performed in triplicates. The error bars represent the standard error of the mean.

sequence have a lower enthalpic barrier ($\Delta H^{\ddagger}$) compared to their swapped counterpart (Figure 3b, P = 0.004; binomial test). Lower values of $\Delta H^{\ddagger}$ for all the PC peptides indicate that the palmitoylation reaction for these peptides is less dependent on temperature than CP peptides. Moreover, all PC peptides have more negative transition state entropies ($\Delta S^{\ddagger}$) than CP peptides (Figure 3c, P = 0.004; binomial test). As a result, the entropic cost ($-T\Delta S^{\ddagger}$) for the palmitoylation reaction is higher for these peptides. The negative entropies also suggest that the transition states for the PC peptides are more ordered than the peptides themselves. On the other hand, the CP peptides show both positive and negative values for entropies (Figure 3c). However, the entropic cost for palmitoylation is still lower when compared to the PC peptides. Such a balanced interplay between entropic and enthalpic contribution to produce a similar free energy barrier, as observed in PC and CP peptide pairs, have also been reported in many previous studies.[41−45]

With these findings, one wonders how critical it is for a proline to be adjacent to the palmitoylated cysteine in order to influence the thermodynamic activation properties of this PTM? We generated a third set of control peptides (listed as shuffled in Table 1) by shuffling the original sequence of each peptide. In the shuffled sequences, we preserved the position of the cysteine and the C-terminal basic residues but ensured that no prolines were adjacent to the S-palmitoylation site. The values of E_a, $\Delta H^{\ddagger}$, $\Delta S^{\ddagger}$, and $\Delta G^{\ddagger}$at 310 K for shuffled peptides are provided in Table 1. In summary, we observed that the free energy of activation ($\Delta G^{\ddagger}$) remains the same for PC, CP, and shuffled sequences. Therefore, the position of proline does not matter overall for the outcome of the autopalmitoylation reaction. No clear trend is observed when comparing $\Delta H^{\ddagger}$ and $\Delta S^{\ddagger}$ between CP and shuffled sequences. However, our results (Figure 3) suggest that proline in the −1 position of cysteine (PC) plays a critical role in lowering the enthalpic barrier of the palmitoylation reaction as PC peptides always had lower values of $\Delta H^{\ddagger}$ compared to CP and shuffled sequences. When examining the position of proline in the 55 peptides that contain either a PC or CP sequence (where the cysteine is palmitoylated), PC occurs in 42 of the 55 peptides. In contrast, when cysteine is not palmitoylated, proline is in the −1 position

DOI: 10.1021/acschembio.5b00429
ACS Chem. Biol. XXXX, XXX, XXX−XXX

for 51% of the peptides showing no preference for the PC sequence. The high frequency of PC in palmitoylated cysteines suggests that the enthalpic differences between sequences may be important for PATs-substrate recognition *in vivo*.

Cysteine Flexibility Influences Palmitoylation. The enthalpic barrier of a reaction is lowered when there is a decrease in enthalpy-driven interaction, causing the system to be more flexible; this increased flexibility, however, increases the entropic barrier for the reaction. To determine if the differences in the enthalpic and entropic barriers observed are due to the changes in the peptide structure depending on the position of the proline relative to the cysteine, we used molecular dynamics to predict the structure of the eight original and the eight swapped counterparts. Figure 4 represents

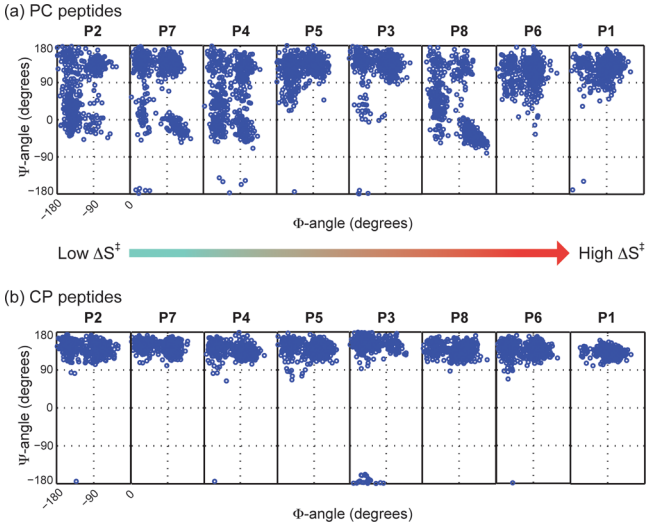

Figure 4. Flexibility of cysteine in PC and CP peptides. (a) Ramachandran plot for PC peptides arranged in increasing order of their entropy of activation ($\Delta S^{\ddagger}$) with leftmost plot representing peptide with more negative entropy of activation. (b) Ramachandran plot for CP peptides corresponding to their PC counterpart. CP peptides are not arranged in increasing order of their activation entropies. All ψ- angles (ordinate) range from −180° to 180°, and all φ- angles (abscissa) range from −180° to 0°.

Ramachandran plots of the cysteine residue for the eight PC peptides and their CP counterparts, in which abscissa and ordinate are φ- and ψ- torsional angles, respectively.

We observe that the PC peptides (Figure 4a) show greater variance in φ- and ψ- torsional angles than CP peptides (Figure 4b), suggesting that the peptide backbone around cysteine residue is more flexible for PC peptides. This observation corroborates the experimental findings (Figure 3b,c), where PC peptides have a lower enthalpic barrier and higher entropic barrier in comparison to CP peptides. In PC sequences, the flexibility of the cysteine residue may increase the energy required for ordering of the transition state (entropic barrier) even though it is easier for the peptide to establish a favorable interaction with Pal-CoA. In contrast, the cysteine residue in a CP peptide precedes a proline residue, and steric hindrance contributed by the bulky side chain of proline may restrict its conformational space and makes it less flexible.[46,47] This potential inflexibility of the cysteine residue in the CP sequence would decrease its entropic barrier but increase its enthalpic barrier, consistent with our experimental results (Figure 3b,c). Furthermore, our results show that there is a correlation between entropy of activation (Figure 3c, white bars) and variance of torsional angles in all eight PC peptides (Figure 4a) with an exception of P8 peptide. Peptides with more negative entropy of activation have greater variance in torsional angles, likely because more energy needs to be expended for the ordering of transition state in the flexible peptides as explained previously. The anomalous behavior of P8 peptide (Figure 4a) can be attributed to the presence of cysteine near the N-terminus.

Sampled trajectories for a majority of the PC peptides form a larger number of clusters; that is, a larger conformational space is sampled (Supplemental Figure S3a). Similarly, solvent accessible surface area (SASA) values, which measure the ability of an atom to interact with a solvent, are higher for cysteine residues in a majority of the PC peptides (Supplemental Figure S3b) consistent with the general trend that the cysteine residue in PC peptides is more accessible for modification compared to in the CP peptide. Figure 5a,b depict

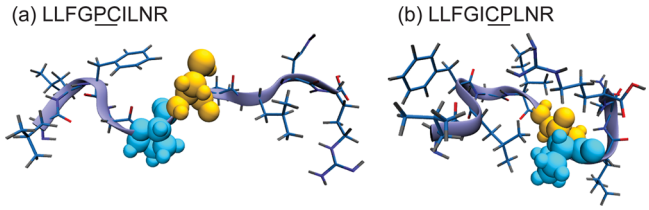

Figure 5. Representative structure obtained from molecular modeling. (a) LLFGPCILNR and (b) LLFGICPLNR. The lowest free energy structure determined from the molecular dynamic simulations is shown. Cysteine and proline are represented by yellow and cyan spheres, respectively.

the low-energy representative structure for LLFGPCILNR and its CP counterpart, respectively. When comparing the two structures, it can be seen that cysteine in peptide LLFPCILNR is exposed, and thus, Pal-CoA may have direct access to the cysteine residue. In the case of its CP counterpart, cysteine is enclosed in a partial cavity surrounded by the side-chains of adjacent alpha-carbon and the proline residue, and is not as exposed. As a result, Pal-CoA might have limited accessibility to the cysteine residue in CP peptides.

CONCLUSION

Our experiments study autopalmitoylation; nevertheless we are able to discern global differences and significant trends in kinetics and activation parameters of palmitoylation based on the order of PC or CP in the peptide. The peptides which contain a proline in the −1 position relative to the S-palmitoylated cysteine have lower enthalpic barriers but higher entropic barriers compared to peptides where proline is in the +1 position or not adjacent to the modified cysteine residue. Free energy of activation, however, is not dependent upon amino acid sequence and shows no significant difference with the change in proline position. With our results, we can postulate that the sequence of the substrate plays a minimal role in palmitoylation *in vivo*, but having a proline at position −1 relative to the modified cysteine (lower enthalpic barrier) is preferred as 42 of 55 experimentally determined palmitoylation sites contain the PC sequence.

Furthermore, we have shown how the position of the proline influences the flexibility of the cysteine residue. We speculate that the structural properties of the modification site, which

DOI: 10.1021/acschembio.5b00429
ACS Chem. Biol. XXXX, XXX, XXX−XXX

govern the activation profile associated with palmitoylation, might be critical for substrate recognition by PATs *in vivo* apart from its sequence. The correlation between the flexibility of the peptide and its entropy and enthalpy of activation, as observed in our study, may also allow us to understand how proline impacts other PTMs. For instance, in phosphorylation, kinases such as MAPKs and CDKs might facilitate phosphorylation by decreasing the enthalpic barrier related to phosphorylation, which is otherwise higher for substrates with proline in +1 position, relative to the modified residue. Similarly, the absence of N-linked glycosylation when an asparagine residue precedes a proline may be due to an increase in enthalpic barrier, caused by the sterically constrained asparagine residue. A high abundance of proline at −1 position in modification sites of O-linked glycosylation also purports to show how lowered enthalpic barrier is favorable for glycosylation.

MATERIALS AND METHODS

S-Palmitoylation Reaction. Palmitoylation reactions were performed in 25 mM sodium-phosphate, 0.1 mM ethylenediaminetetraacetic acid (EDTA), and 0.1 mM tris(2-carboxyethyl)-phosphine (TCEP), pH 8.0 (Reaction buffer). A mixture of 120 μL of reaction buffer and 10 μL of Pal-CoA (5 mM in water) was prepared in a borosilicate culture tube and incubated for 1 h in a water bath at the desired temperature. After prewarming the Pal-CoA mixture, the palmitoylation reaction was initiated by adding 10 μL of peptide solution (1 mM in 60:40 acetonitrile/water (v/v)) to the reaction buffer (molar ratio of 1:5 peptide/Pal-CoA). Aliquots (20 μL) of the reaction mixture were collected at various time points. The collected aliquots were then frozen at −20 °C to quench the reaction. Pal-CoA, TCEP, EDTA, and sodium phosphate were purchased from Sigma-Aldrich.

Sample Preparation for Mass Spectrometry Analysis. Solid-phase extraction, performed with NuTip (Glygen Corp), was used to extract peptides (modified and unmodified) from the aliquots of reaction mixture. Extracted peptides from NuTip were washed four times with water (30 μL) followed by the elution of peptides with two washes in 70:30 acetonitrile/water solution (v/v, 20 μL) and a final wash in 95:5 acetonitrile/water solution (v/v, 20 μL). Ten microliters of water was added to eluted mixture to make the final solution with 70:30 acetonitrile/water (v/v). Formic acid (0.1%) was present in all solutions used for extraction. Mass spectrometric measurements were performed on the final extracted solution. All solvents were obtained from EMD Chemicals.

Data Acquisition. Mass spectra were acquired on a SYNAPT G2 HMDS spectrometer (Waters Corp.) equipped with an electrospray ionization (ESI) source. Peptide solutions were infused using a syringe pump at a flow rate of ∼6 $\mu L \cdot min^{-1}$. The instrument was operated in positive ion mode with capillary voltage of 3.0 kV and sampling cone voltage of 30 V. The temperatures for ion source block and nitrogen desolvation gas were set to be 125 and 250 °C respectively. MassLynx 4.1 software (Waters Corp.) was used for data collection and processing. Spectra were acquired for 1 min with one scan per second over a mass range of m/z 100−1600.

Logarithmic ratio of total counts (monoisotopic peak) for unmodified peptide to sum of total counts (monoisotopic peak) for unmodified and palmitoylated peptide was used to derive rate-constant. The total count of monoisotopic peak for both peptides was multiplied by a correction factor, calculated on the basis of the theoretical mass of the peptide, to account for the contribution from other isotopic peaks of carbon. Our study comes with the internal check for ionization efficiency. The raw signal intensities of unmodified (precursor) and modified (product) varies within the experimental uncertainties, so we assumed the response factor to be unity.

Peptide Selection. Sequences for peptide synthesis were chosen from a previously compiled set of proteins from several species with known palmitoylation target sites, obtained from multiple data sources.[40] From this set, only cysteines that were annotated as being S-palmitoylated and that contained an adjacent proline residue were retained. Tryptic digestion was simulated around the target cysteine of interest and only peptides containing a single cysteine residue were computationally extracted to avoid multiple palmitoylation reactions.

Two types of control peptide sequences were designed. First, proline and the residue at the +1 position (or the −1 position) with respect to cysteine were simply swapped, which essentially replaced a "PC" sequence with a "CP" sequence (or vice versa). Second, a control peptide was designed by shuffling the original sequence such that the positions of the cysteine and C-terminal basic residues were left unchanged, proline was not placed adjacent to the cysteine, and the shuffled peptide was at most 40% identical to the original peptide with a lower likelihood of being palmitoylated. To optimize these constraints, ModPred[40] scores were obtained for each original peptide and its random shuffle. If the difference between the original and shuffled scores was greater than 0.3, that particular shuffle was used to synthesize the control peptide; otherwise, the process was repeated 1000 times until such a shuffle was found. In cases where such a shuffle was not found, the peptide with the greatest difference between the original and shuffled ModPred scores was chosen.

Peptide Synthesis. Peptides were synthesized on an AAPPTec 396 robotic synthesizer (AAPPTec) by standard Fmoc solid-phase synthesis method.[48] A solution of 25:75 piperdine/dimethylformamide (DMF) (v/v) was used for N-terminal deprotection and the coupling cycles were performed using *N*-methyl-2-pyrrolidone (NMP) and 3-(diethoxyphosphoryloxy)-1,2,3-benzotriazin-4(3H)-one (DEPBT) in DMF along with *N*,*N*-diisopropylethylamine (DIPEA). For each synthesis cycle, Fmoc-protected amino acids were added 10-times in excess. After the desired sequences were synthesized, peptides were cleaved from the resin by a mixture containing trifluoroacetic acid (TFA), 2,2′-(ethylenedioxy)-diethanethiol (DET), triisopropylsilane (TIS), thioanisole, and methanol mixed in the ratio of 90:2.5:2.5:2.5:2.5 (v/v/v/v/v). Diethyl ether was used to precipitate and wash the cleaved peptides. Side-chain-protected Fmoc amino acids, Wang-type polystyrene resins, and DEPBT were purchased from AAPPTec. All solvents described above were purchased from EMD Chemicals. All other reagents were purchased from Sigma-Aldrich.

Statistical Analysis. In order to determine if the overall differences between PC and CP peptides were significant, one-tailed binomial tests were used. For each parameter, the number of instances where the PC peptide had a lower mean value than its CP counterpart was counted. The probability (p) assumed under the null hypothesis was 0.5.

Molecular Modeling and Related Analysis. Molecular dynamics simulation for both original and swapped peptides was performed with GROMACS 4.6.5[49] software using the OPLS-AA/L all atom force field.[50] Initial structures for peptides were designed using the PyMOL software.[51] The initial peptide structure was solvated with the TIP3P explicit water model[52] in a dodecahedron box with periodic boundary condition. Sodium chloride was added to solvated system to reach a salt concentration of 100 mM. Energy minimization (EM) was performed in water for 50000 steps using the steepest descents method. Following EM, Ramachandran plots were generated for all the initial structures used. The absence of residues in the outlier region validated the quality of the structure used for the simulation run. EM system was then subjected to two equilibration runs (NVT and NPT) for stabilizing the temperature and pressure of the system. The LINCS[53] algorithm was used to constrain peptide bonds and particle mesh Ewald summation[54] method was used for calculation of electrostatic interactions. Equilibration run was followed by molecular dynamic simulation run for 5 ns in which the trajectories of the peptides were stored every 10 ps. The convergence of potential energy, kinetic energy, pressure, and temperature ensured that the simulation run of 5 ns was sufficient for our system to reach equilibrium. The trajectory file from GROMACS for each time-point was converted into a PDB file and DSSP program was used to calculate φ- and ψ- angles at all time points.[55]

DOI: 10.1021/acschembio.5b00429
ACS Chem. Biol. XXXX, XXX, XXX−XXX

■ ASSOCIATED CONTENT

Supporting Information

The Supporting Information is available free of charge on the ACS Publications website at DOI: 10.1021/acschembio.5b00429.

Table S1 showing peptide sequences that correspond to known palmitoylation sites in different eukaryotic proteins (PDF)

■ AUTHOR INFORMATION

Corresponding Authors

*E-mail: (D.E.C.) clemmer@indiana.edu.
*E-mail: (S.M.) sumukhop@indiana.edu.

Present Address

[‖]Novilytic Laboratories, West Lafayette, Indiana 47906

Notes

The authors declare no competing financial interest.

■ ACKNOWLEDGMENTS

We would like to thank D. Smiley and the DiMarchi Laboratory for assistance with the peptide synthesis and L. Selzer for insightful scientific comments. This work is supported by a grant from the NIH (R01 GM103725) to P.R. and D.E.C.

■ REFERENCES

(1) Karve, T. M., and Cheema, A. K. (2011) Small changes huge impact: the role of protein posttranslational modifications in cellular homeostasis and disease. *J. Amino Acids 2011*, 207691.

(2) Deribe, Y. L., Pawson, T., and Dikic, I. (2010) Post-translational modifications in signal integration. *Nat. Struct. Mol. Biol. 17*, 666−672.

(3) Smotrys, J. E., and Linder, M. E. (2004) Palmitoylation of intracellular signaling proteins: regulation and function. *Annu. Rev. Biochem. 73*, 559−587.

(4) Resh, M. D. (1999) Fatty acylation of proteins: new insights into membrane targeting of myristoylated and palmitoylated proteins. *Biochim. Biophys. Acta, Mol. Cell Res. 1451*, 1−16.

(5) Linder, M. E., and Deschenes, R. J. (2007) Palmitoylation: policing protein stability and traffic. *Nat. Rev. Mol. Cell Biol. 8*, 74−84.

(6) Fukata, Y., and Fukata, M. (2010) Protein palmitoylation in neuronal development and synaptic plasticity. *Nat. Rev. Neurosci. 11*, 161−175.

(7) Lobo, S., Greentree, W. K., Linder, M. E., and Deschenes, R. J. (2002) Identification of a Ras palmitoyltransferase in Saccharomyces cerevisiae. *J. Biol. Chem. 277*, 41268−41273.

(8) Roth, A. F., Feng, Y., Chen, L., and Davis, N. G. (2002) The yeast DHHC cysteine-rich domain protein Akr1p is a palmitoyl transferase. *J. Cell Biol. 159*, 23−28.

(9) Dietrich, L. E., Gurezka, R., Veit, M., and Ungermann, C. (2004) The SNARE Ykt6 mediates protein palmitoylation during an early stage of homotypic vacuole fusion. *EMBO J. 23*, 45−53.

(10) Nadolski, M. J., and Linder, M. E. (2007) Protein lipidation. *FEBS J. 274*, 5202−5210.

(11) Duncan, J. A., and Gilman, A. G. (1996) Autoacylation of G protein alpha subunits. *J. Biol. Chem. 271*, 23594−23600.

(12) Veit, M. (2000) Palmitoylation of the 25-kDa synaptosomal protein (SNAP-25) in vitro occurs in the absence of an enzyme, but is stimulated by binding to syntaxin. *Biochem. J. 345* (Pt 1), 145−151.

(13) Roth, A. F., Wan, J., Bailey, A. O., Sun, B., Kuchar, J. A., Green, W. N., Phinney, B. S., Yates, J. R., 3rd, and Davis, N. G. (2006) Global analysis of protein palmitoylation in yeast. *Cell 125*, 1003−1013.

(14) Martin, B. R., and Cravatt, B. F. (2009) Large-scale profiling of protein palmitoylation in mammalian cells. *Nat. Methods 6*, 135−138.

(15) Bijlmakers, M. J., and Marsh, M. (2003) The on-off story of protein palmitoylation. *Trends Cell Biol. 13*, 32−42.

(16) Salaun, C., Greaves, J., and Chamberlain, L. H. (2010) The intracellular dynamic of protein palmitoylation. *J. Cell Biol. 191*, 1229−1238.

(17) Veit, M., Reverey, H., and Schmidt, M. (1996) Cytoplasmic tail length influences fatty acid selection for acylation of viral glycoproteins. *Biochem. J. 318*, 163−172.

(18) Amici, S. A., McKay, S. B., Wells, G. B., Robson, J. I., Nasir, M., Ponath, G., and Anand, R. (2012) A highly conserved cytoplasmic cysteine residue in the alpha4 nicotinic acetylcholine receptor is palmitoylated and regulates protein expression. *J. Biol. Chem. 287*, 23119−23127.

(19) Moench, S. J., Moreland, J., Stewart, D. H., and Dewey, T. G. (1994) Fluorescence studies of the location and membrane accessibility of the palmitoylation sites of rhodopsin. *Biochemistry 33*, 5791−5796.

(20) Ovchinnikov, Yu. A., Abdulaev, N. G., and Bogachuk, A. S. (1988) Two adjacent cysteine residues in the C-terminal cytoplasmic fragment of bovine rhodopsin are palmitylated. *FEBS Lett. 230*, 1−5.

(21) Sutton, R. B., Fasshauer, D., Jahn, R., and Brunger, A. T. (1998) Crystal structure of a SNARE complex involved in synaptic exocytosis at 2.4 A resolution. *Nature 395*, 347−353.

(22) Turnbull, A. P., Kümmel, D., Prinz, B., Holz, C., Schultchen, J., Lang, C., Niesen, F. H., Hofmann, K. P., Delbrück, H., Behlke, J., et al. (2005) Structure of palmitoylated BET3: insights into TRAPP complex assembly and membrane localization. *EMBO J. 24*, 875−884.

(23) El-Husseini, A. E., Craven, S. E., Chetkovich, D. M., Firestein, B. L., Schnell, E., Aoki, C., and Bredt, D. S. (2000) Dual palmitoylation of PSD-95 mediates its vesiculotubular sorting, postsynaptic targeting, and ion channel clustering. *J. Cell Biol. 148*, 159−172.

(24) Ponimaskin, E., and Schmidt, M. F. (1998) Domain-structure of cytoplasmic border region is main determinant for palmitoylation of influenza virus hemagglutinin (H7). *Virology 249*, 325−335.

(25) Alexander, J., Lim, D., Joughin, B. A., Hegemann, B., Hutchins, J. R., Ehrenberger, T., Ivins, F., Sessa, F., Hudecz, O., Nigg, E. A., Fry, A. M., Musacchio, A., Stukenberg, P. T., Mechtler, K., Peters, J. M., Smerdon, S. J., and Yaffe, M. B. (2011) Spatial exclusivity combined with positive and negative selection of phosphorylation motifs is the basis for context-dependent mitotic signaling. *Sci. Signaling 4*, ra42.

(26) Avruch, J. (2007) MAP kinase pathways: the first twenty years. *Biochim. Biophys. Acta, Mol. Cell Res. 1773*, 1150−1160.

(27) Bause, E. (1983) Structural requirements of N-glycosylation of proteins. Studies with proline peptides as conformational probes. *Biochem. J. 209*, 331−336.

(28) Brown, N. R., Noble, M. E., Endicott, J. A., and Johnson, L. N. (1999) The structural basis for specificity of substrate and recruitment peptides for cyclin-dependent kinases. *Nat. Cell Biol. 1*, 438−443.

(29) Schwarz, F., and Aebi, M. (2011) Mechanisms and principles of N-linked protein glycosylation. *Curr. Opin. Struct. Biol. 21*, 576−582.

(30) Wilson, I. B., Gavel, Y., and von Heijne, G. (1991) Amino acid distributions around O-linked glycosylation sites. *Biochem. J. 275* (Pt 2), 529−534.

(31) Theillet, F.-X., Kalmar, L., Tompa, P., Han, K.-H., Selenko, P., Dunker, A. K., Daughdrill, G. W., and Uversky, V. N. (2013) The alphabet of intrinsic disorder. *Intrinsically Disordered Proteins 1*, e24360.

(32) Radivojac, P., Iakoucheva, L. M., Oldfield, C. J., Obradovic, Z., Uversky, V. N., and Dunker, A. K. (2007) Intrinsic disorder and functional proteomics. *Biophys. J. 92*, 1439−1456.

(33) Velazquez-Dones, A., Hagopian, J. C., Ma, C. T., Zhong, X. Y., Zhou, H., Ghosh, G., Fu, X. D., and Adams, J. A. (2005) Mass spectrometric and kinetic analysis of ASF/SF2 phosphorylation by SRPK1 and Clk/Sty. *J. Biol. Chem. 280*, 41761−41768.

(34) Norris, A. J., Whitelegge, J. P., Faull, K. F., and Toyokuni, T. (2001) Analysis of enzyme kinetics using electrospray ionization mass spectrometry and multiple reaction monitoring: fucosyltransferase V. *Biochemistry 40*, 3774−3779.

(35) Ji, Y., Leymarie, N., Haeussler, D. J., Bachschmid, M. M., Costello, C. E., and Lin, C. (2013) Direct detection of S-palmitoylation by mass spectrometry. *Anal. Chem. 85*, 11952−11959.

DOI: 10.1021/acschembio.5b00429
ACS Chem. Biol. XXXX, XXX, XXX−XXX

(36) Baeza, J., Smallegan, M. J., and Denu, J. M. (2015) Site-specific reactivity of nonenzymatic lysine acetylation. *ACS Chem. Biol. 10*, 122−128.
(37) Deng, L., Kitova, E. N., and Klassen, J. S. (2013) Dissociation kinetics of the streptavidin-biotin interaction measured using direct electrospray ionization mass spectrometry analysis. *J. Am. Soc. Mass Spectrom. 24*, 49−56.
(38) Yang, C., and Compans, R. W. (1996) Palmitoylation of the murine leukemia virus envelope glycoprotein transmembrane subunits. *Virology 221*, 87−97.
(39) Li, M., Yang, C., Tong, S., Weidmann, A., and Compans, R. W. (2002) Palmitoylation of the murine leukemia virus envelope protein is critical for lipid raft association and surface expression. *J. Virol. 76*, 11845−11852.
(40) Pejaver, V., Hsu, W. L., Xin, F., Dunker, A. K., Uversky, V. N., and Radivojac, P. (2014) The structural and functional signatures of proteins that undergo multiple events of post-translational modification. *Protein Sci. 23*, 1077−1093.
(41) Bjelic, S., Brandsdal, B. O., and Aqvist, J. (2008) Cold adaptation of enzyme reaction rates. *Biochemistry 47*, 10049−10057.
(42) Feller, G., and Gerday, C. (2003) Psychrophilic enzymes: hot topics in cold adaptation. *Nat. Rev. Microbiol. 1*, 200−208.
(43) Fields, P. A., and Somero, G. N. (1998) Hot spots in cold adaptation: localized increases in conformational flexibility in lactate dehydrogenase A4 orthologs of Antarctic notothenioid fishes. *Proc. Natl. Acad. Sci. U. S. A. 95*, 11476−11481.
(44) Isaksen, G. V., Aqvist, J., and Brandsdal, B. O. (2014) Protein surface softness is the origin of enzyme cold-adaptation of trypsin. *PLoS Comput. Biol. 10*, e1003813.
(45) Siddiqui, K. S., and Cavicchioli, R. (2006) Cold-adapted enzymes. *Annu. Rev. Biochem. 75*, 403−433.
(46) Hurley, J. H., Mason, D. A., and Matthews, B. W. (1992) Flexible-geometry conformational energy maps for the amino acid residue preceding a proline. *Biopolymers 32*, 1443−1446.
(47) MacArthur, M. W., and Thornton, J. M. (1991) Influence of proline residues on protein conformation. *J. Mol. Biol. 218*, 397−412.
(48) Amblard, M., Fehrentz, J. A., Martinez, J., and Subra, G. (2006) Methods and protocols of modern solid phase Peptide synthesis. *Mol. Biotechnol. 33*, 239−254.
(49) Hess, B., Kutzner, C., Van Der Spoel, D., and Lindahl, E. (2008) GROMACS 4: algorithms for highly efficient, load-balanced, and scalable molecular simulation. *J. Chem. Theory Comput. 4*, 435−447.
(50) Kaminski, G. A., Friesner, R. A., Tirado-Rives, J., and Jorgensen, W. L. (2001) Evaluation and reparametrization of the OPLS-AA force field for proteins via comparison with accurate quantum chemical calculations on peptides. *J. Phys. Chem. B 105*, 6474−6487.
(51) *The PyMOL Molecular Graphics System*, version 1.3; Schrödinger, LLC: New York, 2010.
(52) Jorgensen, W. L., Chandrasekhar, J., Madura, J. D., Impey, R. W., and Klein, M. L. (1983) Comparison of simple potential functions for simulating liquid water. *J. Chem. Phys. 79*, 926−935.
(53) Hess, B., Bekker, H., Berendsen, H. J., and Fraaije, J. G. (1997) LINCS: a linear constraint solver for molecular simulations. *J. Comput. Chem. 18*, 1463−1472.
(54) Essmann, U., Perera, L., Berkowitz, M. L., Darden, T., Lee, H., and Pedersen, L. G. (1995) A smooth particle mesh Ewald method. *J. Chem. Phys. 103*, 8577−8593.
(55) Kabsch, W., and Sander, C. (1983) Dictionary of protein secondary structure: pattern recognition of hydrogen-bonded and geometrical features. *Biopolymers 22*, 2577−2637.

NOTE ADDED AFTER ASAP PUBLICATION

This paper was published ASAP on August 19, 2015, with errors to the SI. The updated SI has been uploaded and reposted on August 21, 2015.

DOI: 10.1021/acschembio.5b00429
ACS Chem. Biol. XXXX, XXX, XXX−XXX